AD-A080 391 CASE WESTERN RESERVE UNIV CLEVELAND OHIO F/G 7/4
OPTICAL AND ELECTROCHEMICAL STUDIES OF ADSORBED TRANSITION META--ETC(U)
MAY 79 E YEAGER, J ZAGAL, B Z NIKOLIC N00014-75-C-0953
UNCLASSIFIED TR-49 NL

(15) N00014-75-C-0953

(12)

OFFICE OF NAVAL RESEARCH

Contract N00014-75C-0953

Task No. NR 359-451

(9) TECHNICAL REPORT NO. 49

(6)

Optical and Electrochemical Studies of Adsorbed Transition Metal Complexes and Their Electrocatalytic Properties.

by

(10) E. Yeager, José Zagal, B. Z. Nikolic and R. R. Adzic

Prepared for Presentation

at the

(14) TR-49

Third Symposium on Electrode Processes

National Meeting, The Electrochemical Society

Boston, Massachusetts - May 6-11, 1979

(12) 30

Case Laboratories for Electrochemical Studies
and The Chemistry Department
Case Western Reserve University
Cleveland, Ohio 44106

(11) May 1979

402 490

SECURITY CLASSIFICATION OF THIS PAGE (When Data Entered)

REPORT DOCUMENTATION PAGE		READ INSTRUCTIONS BEFORE COMPLETING FORM
1. REPORT NUMBER: 49	2. GOVT ACCESSION NO.	3. RECIPIENT'S CATALOG NUMBER
4. TITLE (and Subtitle): Optical and Electrochemical Studies of Adsorbed Transition Metal Complexes and their O_2 Electrocatalytic Properties		5. TYPE OF REPORT & PERIOD COVERED: Technical Report #49 6. PERFORMING ORG. REPORT NUMBER
7. AUTHOR(s): E. Yeager, José Zagal, B.Z. Nikolic and R.R. Adzic		8. CONTRACT OR GRANT NUMBER(s): N00014-75C-0953
9. PERFORMING ORGANIZATION NAME AND ADDRESS: Dept. of Chemistry, Case Western Reserve University, Cleveland, Ohio 44106		10. PROGRAM ELEMENT, PROJECT, TASK AREA & WORK UNIT NUMBERS: NR 359-451
11. CONTROLLING OFFICE NAME AND ADDRESS: Office of Naval Research, Chemistry Program - Chemistry Code 472, Arlington, Virginia 22217		12. REPORT DATE: 1 May 1979 13. NUMBER OF PAGES: 20
14. MONITORING AGENCY NAME & ADDRESS (if different from Controlling Office)		15. SECURITY CLASS. (of this report): Unclassified 15a. DECLASSIFICATION/DOWNGRADING SCHEDULE

16. DISTRIBUTION STATEMENT (of this Report)

This document has been approved for public release and sale; its distribution unlimited.

17. DISTRIBUTION STATEMENT (of the abstract entered in Block 20, if different from Report)

18. SUPPLEMENTARY NOTES

19. KEY WORDS (Continue on reverse side if necessary and identify by block number)

Oxygen electrochemistry, electrocatalysis, transition metal macrocyclics, electrosorption, spectroelectrochemistry

20. ABSTRACT (Continue on reverse side if necessary and identify by block number)

Water soluble transition metal macrocyclics such as the tetrasulfonated phthalocyanines (TSPC) are strongly adsorbed on noble metal and graphite electrodes in acid and alkaline electrolytes. The CoTSPC is a good catalyst for O_2 reduction to peroxide and the FeTSPC for the overall 4-electron reduction. The optical properties of the adsorbed species have been examined using reflectance spectroscopy and evidence obtained for the O_2 adduct with the adsorbed complexes.

DD FORM 1 JAN 73 1473 EDITION OF 1 NOV 65 IS OBSOLETE
S/N 0102-LF-014-6601

Unclassified
SECURITY CLASSIFICATION OF THIS PAGE (When Data Entered)

TABLE OF CONTENTS

A

LIST OF FIGURES

OPTICAL AND ELECTROCHEMICAL STUDIES OF ADSORBED TRANSITION METAL COMPLEXES AND THEIR O_2 ELECTROCATALYTIC PROPERTIES

E. Yeager, José Zagal[a], B. Z. Nikolic[b] and R. R. Adzic[c]
Case Laboratories for Electrochemical Studies
and the Department of Chemistry
Case Western Reserve University
Cleveland, Ohio 44106

ABSTRACT

Water soluble transition metal macrocyclics such as the tetrasulfonated phthalocyanines (TSPC) are strongly adsorbed on noble metal and graphite electrodes in acid and alkaline electrolytes. The CoTSPC is a good catalyst for O_2 reduction to peroxide and the FeTSPC for the overall 4-electron reduction. The optical properties of the adsorbed species have been examined using reflectance spectroscopy and evidence obtained for the O_2 adduct with the adsorbed complexes.

I. INTRODUCTION

The reduction of O_2 at an electrode surface requires a strong interaction of the O_2 molecule with the electrode surface for the reaction to proceed at substantial rates at reasonable potentials (1). One means for obtaining such strong interactions is through the use of transition metal complexes which form O_2 adducts. Various means are available for chemically binding such complexes to stable electrode surfaces. A particularly attractive approach is the *in situ* adsorption of the complex onto the surface. Water soluble transition metal macrocyclics such as the tetrasulfonated phthalocyanines (TSP) are strongly adsorbed at monolayer levels on metals such as Au and Pt and on graphite electrodes in acid and alkaline electrolytes (1-4).

---

a. Present address: Universidat Técnica del Estado, Santiago, Chile.
b. Present address: Faculty of Technology and Metallurgy, University of Belgrade, Belgrade, Yugoslavia
c. Present address: Institute of Electrochemistry, ICTM and Center for Multidisciplinary Studies, University of Belgrade, Belgrade, Yugoslavia

This paper describes electrochemical studies of the cobalt iron tetrasulfonated phthalocyanines adsorbed on graphite and their catalytic properties for O_2 reduction. The electrochemical studies have been complemented with optical specular reflectance measurements of the adsorbed complexes.

II. O_2 INTERACTIONS WITH TRANSITION METAL MACROCYCLIC COMPLEXES

The bonding of O_2 to the transition metal in a macrocyclic complex can involve either lateral or end-on interactions. The Griffiths model (5) (Fig. 1) involves a lateral interaction of the π-orbitals of the O_2 with empty d_{z^2} orbitals of the transition element with back-bonding from at least partially filled d_{xz} or d_{yz} orbitals of the transition element to the π^* orbitals of the O_2. The Vaska complexes (e.g., $Ir(O_2)Cl(CO)(PPh_3)_2$) appear to form such complexes with O_2 (6,7). These compounds are selective oxidation catalysts for cyclic olefins (8). The strong metal-to-oxygen interaction results in a weakening and lengthening of the O-O bond. Sufficiently strong interaction may lead to the dissociative adsorption of O_2 with probably simultaneous proton addition and valency change of the transition element in the manner represented by Pathway I in Fig. 3, followed by reduction of the $M(OH)_2$ to regenerate the catalyst site. Sandstede *et al.* (9-11) have attempted to explain oxygen reduction with square pyramidal Co(II), Fe(II) and Fe(III) complexes on the basis of such π bonding.

With most transition metal complexes the more probable structure for O_2 bonding is the end-on interaction proposed by Pauling (13). The σ-bonding (Fig. 2) can occur through transfer of a metal d_{z^2} electron to the π^* antibonding O_2 molecular orbital with possible retrodative bonding from O_2 π orbitals to metal d orbitals (14,15). The square pyramidal complexes of Fe(II) and Co(II), which have good activity for O_2 reduction, appear to involve such an end-on interaction (16). This adsorption of O_2 is expected to be accompanied by at least a partial charge transfer to yield a superoxide and then peroxide state, as represented by Pathway II in Fig. 3. The adsorption of the O_2 on the square pyramidal complexes of Fe(II) and Co(II) may lead directly to the superoxide state. With somewhat similar oxyhemoglobin complexes of iron, various workers have proposed that O_2 binding to the iron involves O_2^- or $O_2^=$ states with Fe in the III valent state (17,18). The change in valency state of the transition metal coupled with the change in O_2 oxidation state during formation of the O_2 adduct corresponds in principle to the redox electrocatalyst concept proposed by Beck *et al.* (19,20).

The further reduction of the O_2 beyond the peroxide state requires rupture of the O-O bond. Such can occur in Pathway IIB through the formation of $O^{\cdot-}$ or $HO\cdot$ free radicals in solution or the simultaneous reduction-bond cleavage (electrochemical desorption) to

yield H_2O or OH^-. Neither of these processes is likely to be sufficiently fast at practical operating potentials for O_2 cathodes but the electrochemical desorption is a better candidate. The free energies of formation of the $O^{\cdot}$ and $OH^{\cdot}$ free radicals in solution are just too high to achieve sufficient concentrations of these species for the subsequent homogeneous reactions to proceed at rates corresponding to reasonable current densities at acceptable electrode potentials.

Pathway III in Fig. 3 provides an alternate means for bringing about rupture of the O-O bond through the formation of an -O-O- bridge. Such a mechanism may come into play with the proper spacing of transition metal elements in a bimetal complex such as a macrocycle. The formation of the bridge species also requires that the two metal species have partially filled d-orbitals to participate in bonding with the π^* orbitals of the oxygen. Macrocyclic transition metal complexes of the type $M\text{-}O_2\text{-}M$ have been synthesized (e.g., ref. 21-23) and appear to occur naturally in hemeythrin. Various solution phase macrocyclics including the tetrasulfonated phthalocyanines (M-TSP) have been reported to form O_2 complexes of the type $M\text{-}TSP\cdot O_2\cdot M\text{-}TSP$ (26-32) where M is Co or Fe.

For any of the mechanisms in Fig. 2 considerable questions exist as to the reversibility of the O_2 adsorption step at the rather high rates involved with practical O_2 cathodes. For O_2 to bond to M^z will generally require the replacement of a water molecule or anion of the electrolyte -- a situation which would normally be expected to be unfavorable to O_2 unless the O_2 adduct has a pronounced dipolar character ($M^{z+1}O\text{-}O^-$) (24,25).

III. PRIOR STUDIES OF O_2 REDUCTION ON TRANSITION METAL MACROCYCLIC COMPLEXES

Metal phthalocyanines have been found to have catalytic activity for the heterogeneous O_2 reduction (1,2,20,33-39). A direct correlation has been found (20,34,35) between the first oxidation potential of the metal phthalocyanine and catalytic activity for O_2 reduction. Beck (20) has proposed a mechanism based on data for O_2 reduction on Co tetraazaannulene (Co-TAA) which gives Tafel slopes of -60 mV/decade in acid solution. This author proposed that the metal complex reacts with oxygen according to the reaction:

$$M^{II} + O_2 \xrightarrow{H^+} M^{III} - O_2H \qquad (a)$$

where O_2 undergoes partial reduction with simultaneous oxidation of the metal center. The O_2 adduct, according to Beck, then undergoes a 2-electron reduction as the rate determining step, regenerating the catalyst. For a transfer coefficient $\alpha = 0.5$, the Tafel slope could then be -60 mV/decade. Simultaneous 2-electron steps, however, are

unlikely on energetic grounds.

On the basis of O_2 reduction data on Fe phthalocyanines, Appleby and Savy (36,39) propose that the rate-determining step is the breaking of the O-O bond with the mechanism:

$$O_2 \rightleftharpoons O_{2\,ads} \qquad (b)$$

$$O_{2\,ads} + H_2O + e^- \rightleftharpoons O_2H_{ads} + OH^- \qquad (c)$$

$$O_2H_{ads} + e^- \rightleftharpoons O_2H^-_{ads} \qquad (d)$$

$$O_2H^-_{ads} + H_2O \longrightarrow 2\,OH^-_{ads} + OH^- \qquad (e)$$

IV. EXPERIMENTAL PROCEDURES

The present work has involved water soluble tetrasulfonated phthalocyanine adsorbed on graphite substrates (2,40). The redox properties of the catalysts have been examined using cyclic voltammetry. This approach has been facilitated by use of the basal plane of stress-annealed pyrolytic graphite (SAPG) with x-ray diffraction rocking angles as small as $\Delta\theta_{\frac{1}{2}} = 0.4^o$. This material has low background current (41) and very little activity for the O_2 reduction process (42). The O_2 reduction studies have been carried out with the rotating disk-ring electrode technique.

A disk electrode exposing the basal plane of SAPG (2) with an area of 0.20 cm^2 was used for the rotating disk measurements. For the ring-disk measurements, the disk was constructed with ordinary pyrolytic graphite (OPG) ($\Delta\theta_{\frac{1}{2}} = 45^o$, radius = 0.250 cm) with Au (99.99% pure) as the ring (inner radius = 0.272 cm, outer radius = 0.357 cm). The fragile nature of the SAPG prevented its use as the disk in the ring-disk experiments. Unless otherwise indicated, all measurements on SAPG and OPG were on the basal planes.

The Teflon cell had separate compartments for the reference (saturated calomel-SCE) and counter electrode (Au-foil) with an addition isolation compartment between the working and reference compartments. A Teflon Luggin capillary was used to minimize IR drop. All measurements were made at 20 to 22°C.

The surface of the basal plane of SAPG was renewed by use of the adhesive tape technique with care to avoid contamination of the Teflon mounting with the adhesive of the tape (2,42). The OPG electrodes were polished using 0.3μ alumina. The M-TSP was adsorbed on the graphite surface by placing a drop of solution of the complex (10^{-3} M) on the electrode. The electrode was subsequently washed with

purified water. For experiments in acid solution some of the complex was added to the electrolyte to preserve the adsorbed catalyst layer during the measurements. In the other solutions the adsorption was sufficiently strong to render the loss of the adsorbed complex negligible over the duration of the measurements.

Basic (0.1M NaOH) and acid (0.05M H_2SO_4) solutions were prepared as described before (2). Solutions of pH were as follows: 1M NaOH: pH = 13.8; 0.1M NaOH: pH = 12.9; 0.1M Na_2CO_3: pH = ~1.5; 0.005M Na_2CO_3 + 0.05M Na_2SO_4: pH = 10.8; 0.0015M NaOH + 0.05M H_3BO_3 + 0.05M Na_2SO_4: pH = 8.7; 0.10M NaOH + 0.05M H_3BO_3 + 0.05M Na_2SO_4: pH = 6.3 and 0.1M NaH_2PO_4; pH = 4.4. Special precautions were taken to minimize $CO_3^{=}$ in the alkaline electrolytes. The Co-TSP and Fe-TSP were prepared and purified by the procedures described by Weber and Busch (43).

V. RESULTS

A. Voltammetry of Adsorbed Co-TSP and Fe-TSP

Figure 4 shows the voltammetry curves obtained at different potential scan rates for Co-TSP pre-adsorbed on the basal plane of SAPG. A Teflon hood (44) was used to eliminate edge effects and leakage of the electrolyte between the Teflon and the side of the disk electrode, which otherwise cause a pronounced slant to the voltammetry curves. The charge under the peak is 3 $\mu C/cm^2$, which corresponds to a surface concentration of 3×10^{-11} moles/cm^2 of adsorbed metal complex assuming a one-electron process. Assuming that the surface redox couple obeys the Nernst equation, the peak current is given by

$$i_p = \frac{n^2 F \Gamma \nu}{4RT} \qquad (1)$$

where Γ is the surface concentration, ν is the potential scan rate and n is the number of electrons per adsorbed molecule. The charge under the peak is equal to $Q = nF\Gamma$. Experimental values of i_p and Q give n = 0.9, indicating that one electron is involved in the surface redox process, which is likely (45,46), i.e.,

$$(Co^{II}TSP)_{ads} \rightleftharpoons (Co^{III}TSP)_{ads} + e^- \qquad (f)$$

For Co-TSP adsorbed on OPG, the charge from cyclic voltammetry is ~ 13 $\mu C/cm^2$ or ~ 4 times that of SAPG.

The Fe-TSP also readily adsorbed on SAPG as evidenced by the voltammetry curve (Fig. 5). From the scan rate dependence of both peaks I and II, a one-electron transfer is involved in each case. The charge under each peak estimated from the area between the solid

and dotted lines is ~3.0 $\mu C/cm^2$ for SAPG and ~13 $\mu C/cm^2$ for OPG, which are the same as for Co-TSP. (The charge is independent of ν over the range 50 to 1000 mV/s.) This suggests that the surface coverages by Co-TSP and Fe-TSP species are essentially the same.

Peak I exhibits a pH dependence of 0.057 V/pH over the pH range 4.5 to 13 (Fig. 6). This peak is believed to involve the Fe(III)-TSP/Fe(II)-TSP couple. The pH dependence probably results from hydrolysis of the Fe(III) state (47,48). The redox reaction can then be written as

$$Fe^{III}OH + H_2O + e^- \rightleftharpoons Fe^{II}OH_2 + OH^- \qquad (g)$$

The position of peak II shifts with pH only at low pH values. It is not sure what process is involved for this reversible peak. Perhaps in the reduced form the electron is delocalized in the π system of the macrocyclic ligand or alternatively the Fe is in the equivalent of the I state. Lever and Wilshire (49) have reported that iron(II) phthalocyanine can be electrochemically reduced in non-aqueous solvents to give Fe(I)-Pc.

B. O_2 Reduction on Adsorbed Co-TSP

The rotating ring-disk data for O_2 reduction on Co-TSP/OPG in 0.1M NaOH are shown in Fig. 7. Using these data and the analysis of Wroblowa *et al.* (50), the O_2 reduction has been found to proceed through parallel processes with the reduction to the peroxide predominant and the overall 4-electron reduction minor (51). The usual rotating disk plots of $1/i$ vs. $1/\sqrt{\omega}$ also yield slopes, B, very close to those expected for a process yielding 2 electrons per O_2 diffusing through the boundary layer ($B = 1.40 \times 10^2$ mA(rpm)$^{-\frac{1}{2}}$ as compared with a theoretical value (54) of 1.42×10^2 mA(rpm)$^{-\frac{1}{2}}$ in 0.1M NaOH.) Fig. 8 indicates rate constants evaluated from the rotating disk-ring data for the two parallel processes:

$$O_2 + 2H_2O + 4e^- \xrightarrow{k_1} 4OH^- \qquad (h)$$

$$O_2 + H_2O + 2e^- \xrightarrow{k_2} HO_2^- + OH^- \qquad (i)$$

The corresponding Tafel slopes are $(\partial \ln k_1/\partial E) = -0.15$ V/decade and $(\partial \ln k_2/\partial E) = -0.12$ V/decade. These slopes suggest that the first electron transfer is rate controlling for each pathway.

C. O_2 Reduction on Adsorbed Fe-TSP

Rotating ring-disk electrode data for Fe-TSP adsorbed on OPG are shown in Fig. 9 for 0.1M NaOH. The ring current was measured at the diffusion limiting HO_2^- oxidation condition. The ring currents for disk potentials more positive than -0.32 V are zero, which indicates that the O_2 reduction occurs via 4 electrons with

no detectable peroxide at those potentials. The small amount of HO_2^- detected at higher polarizations may be due in part to O_2 reduction on zones of the graphite not covered by Fe-TSP. The maximum in the disk current for the OPG substrate occurs almost at the same potential as for the Fe-TSP/OPG. The maximum in the disk current for the latter, however, is far too pronounced to be caused just by a substrate background current. This maximum for Fe-TSP/OPG correlates well with peak I in the voltammetry curve (Fig. 5). The analysis of the ring-disk currents at potentials cathodic to -0.45 V indicates a large potential dependence for the ratio of disk-to-ring current at infinite rotation rate and hence parallel mechanisms appear operative.

Tafel plots for O_2 reduction on Fe-TSP/OPG in solutions of various pH are shown in Fig. 10. The diffusion limiting current densities for the 4-electron O_2 reduction are tabulated in the figure. The currents are first order in O_2 concentration over the entire potential range. The lower linear Tafel region is pH dependent with slopes $\sim$ -35 mV/decade at pH 10.8 - 13.9 and increasing to -65 mV/decade at pH 4.4. Reproducible data could not be obtained at pH below 4 because the adsorbed Fe-TSP decomposed when the potential was scanned to more cathodic potentials in acid electrolytes. This decomposition is accelerated by the presence of O_2 and is probably caused by HO_2^- formation. Reaction order studies with respect to OH^- indicated that the reaction is <u>inverse</u> first order in OH^- at pH 10 to 3.8 and approaches zero order at lower pH (see Fig. 11). This correlates with the increase in Tafel slope at lower pH in Fig. 10.

The apparent limiting current at $I/(I_L-I)$ values of $\sim$0.8 is particularly interesting. This current is not diffusion controlled and is first order in O_2 concentration but independent of pH over the entire range studies. It is associated with the pre-wave in Fig. 9. A chemical limiting process with potential insensitive kinetics is involved.

Only rotating disk experiments were carried out on Fe-TSP adsorbed on SAPG (Fig. 12), but the behavior is similar to that on Fe-TSP/OPG. The 1/i vs. $1/\sqrt{\omega}$ plots indicate that at potentials anodic to -0.5 V, O_2 reduction proceeds virtually entirely by the overall 4-electron process without the generation of peroxide. At more cathodic potentials, these plots indicate substantial peroxide generation. This is not peroxide generation on bare portions of the SAPG surface since O_2 reduction to either peroxide or OH^- is grossly inhibited on the basal plane in the absence of the adsorbed complexes (42).

The current-potential data can be deconvoluted into two component processes as shown in Fig. 13. The process corresponding to i_b has been assumed to follow Tafel linearity only at more cathodic potentials and to approach zero current at potentials negative to the

reversible value for the overall 4-electron reduction in order to fit the experimental data. Such behavior may occur if process b corresponds to a hydrogen peroxide producing reaction with the bulk peroxide concentration finite but low (e.g., 10^{-7} M). Small residual currents were observed on the ring after several cathodic potential sweeps, providing evidence for such peroxide. The curve corresponding to i_b then approaches the reversible potential for the O_2/HO_2^-, OH^- couple for whatever is the bulk concentration of HO_2^-.

D. Specular Reflectance Studies of Adsorbed Co-TSP and Fe-TSP

Specular reflectance measurements have been carried out for Co-TSP and Fe-TSP adsorbed on the basal plane of SAPG, Au and Pt. The apparatus and techniques will be described in a separate publication (53). The Pt and Au surfaces were optically polished with Al_2O_3 while fresh SAPG surfaces were prepared with the adhesive tape technique. The reflectance changes were recorded from 420 to 700 mm at 45° angle of incidence with both perpendicular and parallel polarization.

The reflectance spectra for Co-TSP on Pt are shown in Fig. 14 for both acid and alkaline electrolytes with and without O_2 present. Figure 14 presents comparable data for Fe-TSP adsorbed on SAPG and Pt in 0.1M NaOH. These spectra are believed to represent the first time that the O_2 adducts of Fe-TSP and Co-TSP adsorbed on surfaces have been observed. The transmission absorption spectra for the Co-TSP and Fe-TSP in O_2 saturated alkaline and acid solutions, measured in the present study (53), also indicate the formation of O_2 adducts in solution, including the adduct M-TSP-O_2-M-TSP. The spectral changes associated with the formation of the O_2 adduct with the adsorbed Co-TSP and Fe-TSP are similar to those occurring with the formation of the corresponding O_2 solution phase adducts in acid and alkaline solutions.

The configuration of the adsorbed complex relative to the surface is not fully clear. The most likely configuration is with the macrocyclic structure parallel to the surface and with the transition metal interacting with the surface through an -O- linkage. Such a configuration would not easily provide for -O-O- bridging between transition metal sites with two adjacent complexes or between one metal site and the carbon surface. It is unlikely that the M-TSP complexes are adsorbed on the electrode surfaces with the macrocyclic ligand parallel and immediately adjacent to the surface (i.e., in the inner Helmholtz plane). The peaks in the 600-680 nm range for the adsorbed species occur at nearly the same wavelengths as for the bulk solution species. On the other hand, the π-π^*

parallel transition is sensitive to the immediate dielectric environment adjacent to the macrocyclic ligand and would be perturbed by the interaction with the graphite π orbitals or metal orbitals if in direct contact with the surface. An alternative possibility is that these macrocyclic complexes are edge-on adsorbed with the sulfonate groups interacting with the surfaces. This arrangement would facilitate -O-O- bridging.

Further UV-visible reflectance studies using polarized light and Raman studies are planned to gain more information concerning how these species are adsorbed.

VI. MECHANISTIC CONSIDERATIONS OF O_2 REDUCTION ON ADSORBED Co-TSP and Fe-TSP

The O_2 reduction to peroxide on Co-TSP/graphite may proceed according to the following scheme:

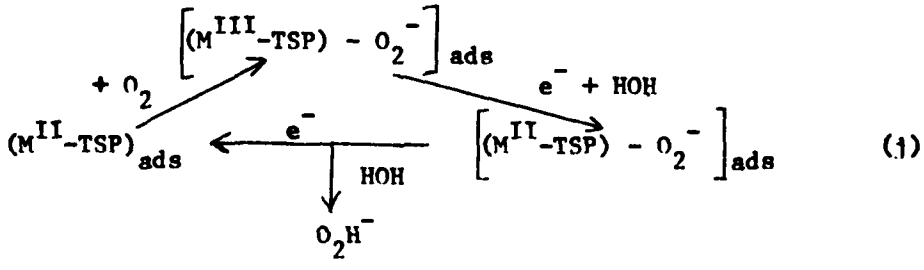

(1)

where the first step is probably ligand displacement (water or OH^- groups, depending on pH), followed by a heterogeneous electron transfer to yield the peroxide with this step rate controlling.

The more cathodic peak in the voltammetry curves for Fe-TSP (Peak II in Fig. 5) occurs at potentials in the lower polarization region (Fig. 10) where deviations from Tafel linearly become evident. This suggests an involvement of the $(Fe(III)OH\ TSP)_{ads}/(Fe(II)TSP)_{ads}$ couple in the reaction mechanism responsible for current component i_a. The following mechanism explains the behavior of this component for pH > 8:

$$(Fe^{III}{}_{OH\text{-}TSP})_{ads} + e^- \underset{}{\overset{k_1}{\rightleftharpoons}} (Fe^{II}\text{-}TSP)_{ads} + OH^- \qquad (k)$$

$$(Fe^{II}\text{-}TSP)_{ads} + O_2 \overset{k_2}{\rightleftharpoons} (Fe^{III}\text{-}O_2^-\text{-}TSP)_{ads} \qquad (l)$$

$$(Fe^{III}\text{-}O_2^-\text{-}TSP)_{ads} + e^- \xrightarrow{k_3} \text{intermediates} \qquad (m)$$

with reaction m normally rate controlling. On the basis of the kinetic evidence, the pathway appears to involve only one adsorbed M-TSP complex at a time, and therefore, not a bridge between the transition metal centers in two complexes. The possibility exists for -O-O-

bridging between the surface and the transition metal but this seems unlikely.

In the lower Tafel linear region, reaction m is rate controlling while the limiting current $(i_a)_L$ is associated with reaction 1 becoming controlling. The corresponding kinetic equation is (50,51)

$$i_a = (i_a)_L \frac{(OH^-)^{-1} K \exp -(1+\alpha)\frac{F}{RT}(E-E_o)}{[1 + (OH^-)^{-1} \exp -\frac{F}{RT}(E-E_o)][1 + K \exp -\frac{\alpha F}{RT}(E-E_o)]} \quad (2)$$

where $(i_a)_L = 4 Fk_2(O_2)m$ (3)

with m the surface concentration of Fe-TSP, E_o the standard electrode potential for reaction m, α the transfer coefficient for this step, $K = k_3/k_{-2}$, and (OH^-) and (O_2) the OH^- and O_2 concentrations.

This equation predicts the essential features of the experimental data below the high polarization-Tafel linear region in the pH range from 8.7 to 13.8; i.e. the reaction rate is first order in (O_2) and -1 in (OH^-), and predicts a limiting current density $(i_a)_L$ which is directly proportional to O_2 concentration, to Fe-TSP surface concentration and independent of pH. The quantity $(i_a)_L$ is due to a potential insensitive chemical process, reaction 1, which becomes rate controlling when the Fe(II)-TSP species approach saturation and the cathodic polarization has increased the rate of reaction m to a relatively high value. According to this proposed mechanism, the Tafel slope for the linear Tafel region of i_a should be $-RT/((1+\alpha)F)$. The value of the slope will depend on the value of α. For $\alpha = 0.5$ the slope is $-RT/(1.5F)$ or -40 mV/decade and for $\alpha = 1$ is $-RT/(2F)$, or -30 mV/decade, as compared with an experimental value of $\sim$ -35 mV/decade.

At more acidic pH it is necessary to consider the acid-base equilibrium:

$$Fe^{III}OH^- \overset{K_B}{\rightleftharpoons} Fe^{III} + OH^- \quad (o)$$

The redox process may be represented as

$$\begin{array}{ccc} Fe^{III}OH & \rightleftharpoons & Fe^{II} + OH^- \\ \uparrow\downarrow K_B & \nearrow e^- & \\ Fe^{III} + OH^- & & \end{array} \quad (p)$$

with the TSP ligand not shown. The mechanism can then be modified for low pH (< 8) by replacing reaction k by reaction p followed with

reaction 1 as rate controlling. The current component i_a is then

$$i_a = 4Fk_2(Fe^{II})(O_2) \tag{4}$$

and, taking into account reaction p and considering low pH (< 4), becomes

$$i_a = (i_a)_L \frac{K_B^{-1} \exp -\frac{F}{RT}(E-E_o)}{1 + K_B^{-1} \exp -\frac{F}{RT}(E-E_o)} \tag{5}$$

This equation fits the experimental observation that at low pH i_a has relatively little or no pH dependence (see Fig. 11). These two mechanisms are expected to be competitive in the pH range between 10 and 4. This would explain the gradual change in the Tafel slope from -30 mV/decade to -60 mV/decade.

At high cathodic polarization, the O_2 reduction mechanism probably reverts to a pathway similar to that proposed for the Co-TSP/graphite system (reaction j).

VII. IMPLICATIONS OF RESEARCH

Some transition metal macrocyclics such as the adsorbed Fe-TSP are active catalysts for the overall 4-electron reduction of O_2. The kinetics, however, are reasonably well explained by pathways which do not involve bridged -O-O- adducts and are first order rather than second order with respect to the surface concentrations of Fe-TSP. The reflectance spectra indicate the formation of O_2 adducts with the adsorbed Co-TSP and Fe-TSP but these spectra also do not provide any specific evidence for bridged -O-O- adducts.

The most critical feature of the 4-electron reduction appears to be the location of the potential for the Fe(II)-TSP/Fe(III)-TSP couple at a value near that at which the O_2 reduction occurs. The pH dependence of this potential, however, is such that the catalytic activity for the 4-electron reduction is depressed with increasing OH^- ion concentration. On the other hand, the 2-electron reduction to the peroxide is essentially independent of OH^- activity. As a consequence, in the concentrated bases used in most fuel cell and air battery applications, the peroxide generation becomes significant even at low current densities and this in turn leads to accelerated attack of the Fe-TSP as well as the graphite or carbon surfaces.

ACKNOWLEDGMENT: This research has been supported by the Office of Naval Research (optical studies) and the Department of Energy through a subcontract from the Diamond Shamrock Corporation (O_2 re-

duction studies). One of the authors (JZ) has held a fellowship from the Organization of American States during part of this work, while a second (BZN) held a postdoctoral fellowship from the Research Fund of the Socialistic Republic of Serbia, Yugoslavia during part of this work.

REFERENCES

1. R. K. Sen, J. Zagal and E. Yeager, Inorg. Chem., 16, 3379 (1977).

2. J. Zagal, R. K. Sen and E. Yeager, J. Electroanal. Chem., 83, 207 (1977).

3. A. P. Brown, C. Koval and F. C. Anson, ibid., 72, 379 (1976).

4. M. Brezina, W. Khalil, J. Koryta and M. Mugilova, ibid., 77, 237 (1977).

5. J. S. Griffiths. Proc. Roy. Soc. (A), 235, 73 (1956).

6. N. W. Terry, E. L. Amma, and L. Vaska, J. Amer. Chem. Soc., 94, 653 (1972).

7. L. Vaska, Science, 140, 809 (1963).

8. J. Collman, M. Kubola and J. Hosking, ibid., 89, 4809 (1967).

9. M. Behret, M. Binder, W. Clauberg and G. Sandstede, Extended Abstracts, International Electrochemical Society Meeting, Zurich, Switzerland, 1976. Abst. No. 230.

10. M. Behret, W. Clauberg and G. Sandstede, Ber. Bunsenges. Phys. Chem., 81, 54 (1977).

11. H. Alt, H. Binder, W. Linder and G. Sandstede, in "From Electrocatalysis to Fuel-Cells," Seattle, Univ. of Washington Press, 1971.

12. E. Yeager, "Mechanisms of Electrochemical Reactions on Non-Metallic Surfaces," in Electrocatalysis on Non-Metallic Surfaces, NBS Special Publication 455, 1976, pp. 203-219.

13. L. Pauling, Nature, 203, 182 (1964).

14. D. M. Mingos, Nature, 230, 154 (1971).

15. E. I. Ochiai, J. Inorg. Nucl. Chem., 35, 3375 (1974).

16. See e.g. B. Hoffman, D. Diemente, and F. Basolo, J. Amer. Chem. Soc., 92, 61 (1970).

17. J. J. Weiss, Nature, 203, 183 (1964).

18. E. F. Ochiai, J. Inorg. Chem., 36, 2129 (1974).

19. F. Beck, Ber. Bunsenges. Phys. Chem., 77, 353 (1973).

20. F. Beck, J. Appl. Electrochem., 7, 239 (1977).

21. E. I. Ochiai, Inorg. Nucl. Chem. Letters, 10, 453 (1974).

22. M. J. Bennett and P. B. Donaldson, J. Amer. Chem. Soc., 93, 3307 (1971).

23. W. P. Schaefer, Inorg. Chem.,7, 725 (1968).

24. H. C. Stynes and J. A. Ibers, Inorg. Chem., 94, 5125 (1972).

25. W. Brimgar, C. Chang, J. Gerbel and T. Traylor, Inorg. Chem., 96, 5597 (1974).

26. D. Vonderschmitt, K. Bernauer and S. Fallab, Helv. Chim. Acta, 48, 951 (1965).

27. J. Weber and D. H. Busch, Inorg. Chem., 4, 469 (1965).

28. J. Veprek-Siska, E. Schwertnerova and D. M. Wagnerova, Chimia, 26, 75 (1972).

29. F. L. Joe, Ph.D. Thesis, The George Washington University, 1976.

30. L. C. Gruen and R. J. Blagrove, Aust. J. Chem., 26, 319 (1973).

31. E. Schwertnerova, D. M. Wagnerova and J.Veprek-Siska, Z. Chem., 14, 311 (1974).

32. D. M. Wagnerova, E. Schwertnerova and J. Veprek-Siska, Coll. Czech. Chem. Comm., 39, 1980 (1974).

33. H. Jahnke, M. Schönborn and G. Zimmermann in "Organic Dyestuffs as Catalysts for Fuel-Cells," Topics in Current Chemistry, 61, 135 (1976).

34. J. Manassen and Bar-Ilan, J. Catalysis, 17, 86 (1970).

35. J. P. Randin, Electrochim. Acta, 19, 83 (1974).

36. A. J. Appleby and M. Savy, Natl. Bur. Stand. Spec. Publ., 455,

241 (1976).

37. A. J. Appleby, J. Fleisch and M. Savy, J. Catal., 44, 281 (1976).

38. A. J. Appleby and M. Savy, Electrochim. Acta, 22, 1315 (1977).

39. A. J. Appleby and M. Savy, in Proc. Symp. Electrode Materials and Processes for Energy Conversion and Storage, J.D.E. McIntyre, S. Srinivasan and F. W. Will, eds., pp. 247-264, 1977.

40. J. Zagal, P. Bindra and E. Yeager, "Oxygen Reduction on Metal Phthalocyanines Adsorbed on Graphite Electrodes," Paper 539, National Meeting, The Electrochemical Society, Seattle, May 21-6, 1978.

41. J. P. Randin and E. Yeager, J. Electroanal. Chem., 36, 257 (1972).

42. I. Morcos and E. Yeager, Electrochim. Acta, 15, 953 (1970).

43. J. Weber and D. H. Busch, Inorg. Chem., 4, 469 (1965).

44. J. P. Randin and E. Yeager, J. Electrochem. Soc., 118, 711 (1971).

45. F. Beck, Ber. Bunsenges., 77, 353 (1973).

46. J. Manassen, J. Catal., 33, 133 (1974).

47. H. Sigel, P. Waldmeir and B. Prijs, Inorg. Nucl. Chem. Letters, 7, 161 (1971).

48. K. Fenkart and C. H. Brubaker, J. Inorg. Nucl. Chem., 3245 (1968).

49. A.B.P. Lever and J. P. Wilshire, Inorg. Chem., 17, 1145 (1978).

50. H. S. Wroblowa, Y. C. Pan and G. Razumney, J. Electroanal. Chem., 71, 195 (1976).

51. J. Zagal, Ph.D. Thesis, Case Western Reserve University, 1978.

52. J. Zagal, P. Bindra and E. Yeager, J. Electrochem. Soc., to be submitted.

53. B. Z. Nikolic, R. R. Adzic, and E. Yeager, J. Eâectroanal. Chem., submitted for publication.

54. See eq. 2 in ref. 2 and the discussion therein.

Figure 1. Interaction of π and π^* molecular orbitals of O_2 with d orbitals of a metal in Griffiths model.

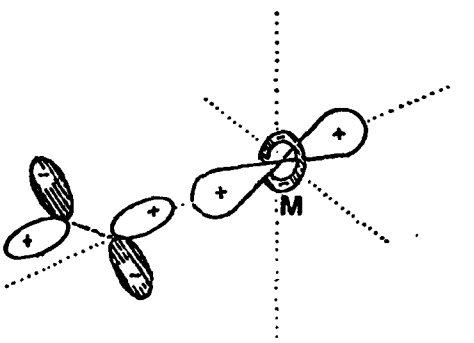

Figure 2. Interaction of π^* molecular orbital of O_2 with d_{z^2} orbital of a metal in Pauling model.

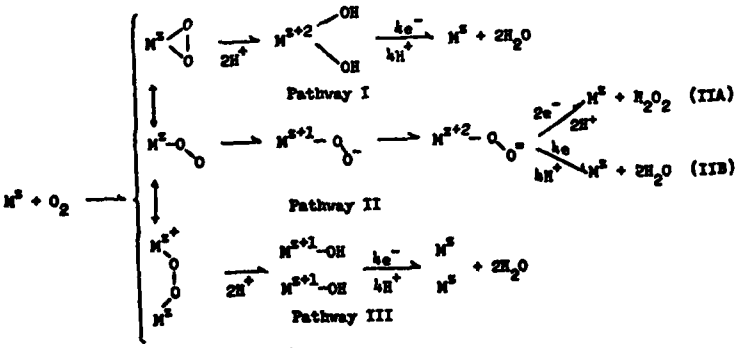

Figure 3. Reaction pathways for O_2 electroreduction in acid electrolytes (Yeager (12)).

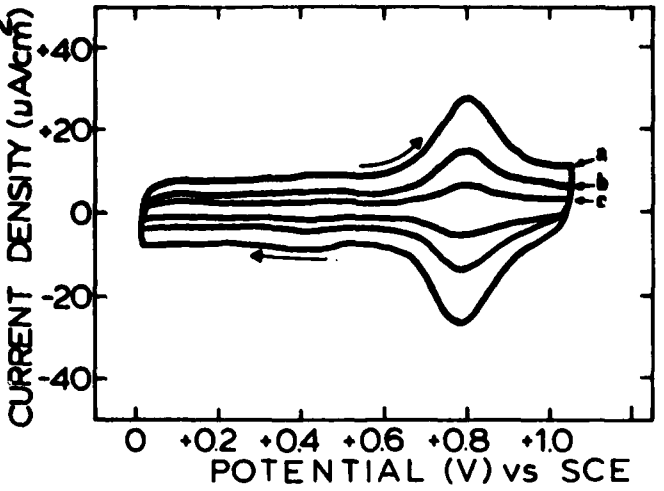

Figure 4. Cyclic voltammograms at different scan rates for Co-TSP adsorbed on SAPG. Electrolyte: 0.05M H_2SO_4. (No Co-TSP in solution; obtained with hood to block electrolyte at edge of disk).

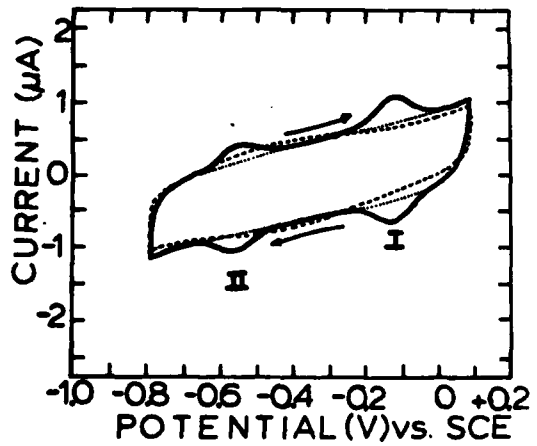

Figure 5. Cyclic voltammogram with (solid line) and without (dashed line) Fe-TSP pre-adsorbed on SAPG. Supporting electrolyte: 0.1M NaOH, He saturated. Scan rate: 500 mV/s (obtained without hood).

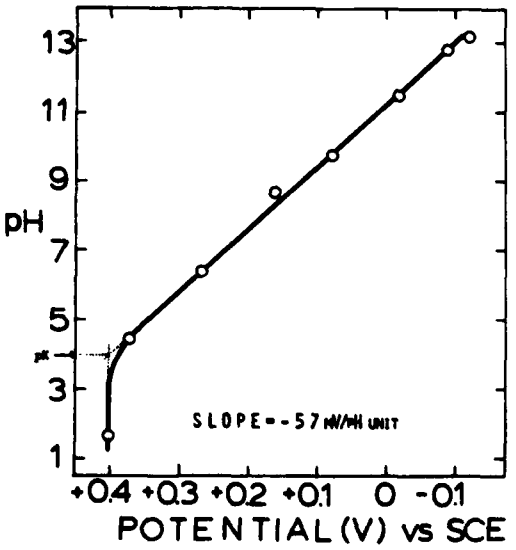

Figure 6. pH dependence of the potential of peak 1 in the voltammetry (see Fig. 5) for Fe-TSP adsorbed on OPG.

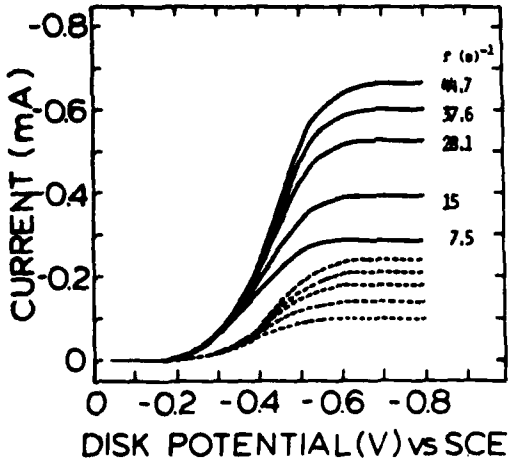

Figure 7. Rotating ring-disk data for O_2 reduction on Co-TSP pre-adsorbed on OPG in 0.1M NaOH. Disk current indicated by solid lines; ring current by dashed lines. Scan rate: 10m V/s. Ring potential: +0.1V vs SCE. Ring currents are anodic. Collection efficiency: N = 0.38.

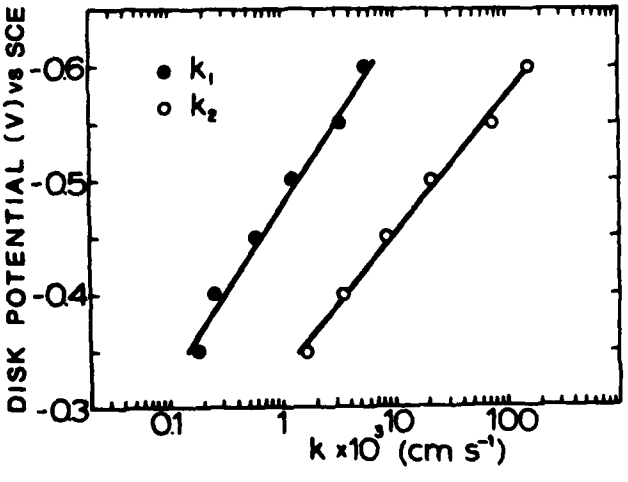

Figure 8. Potential dependence of the heterogeneous rate constants for the $4e^-$ reduction (k_1) and $2e^-$ reduction (k_2) of O_2 on Co-TSP adsorbed on OPG in 0.1M NaOH.

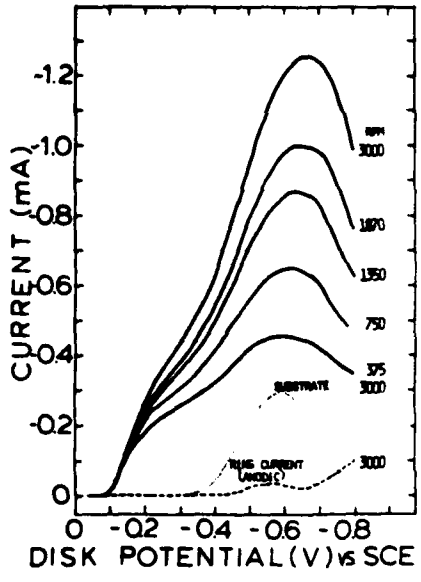

Figure 9. Rotating ring-disk data for O_2 reduction on Fe-TSP pre-adsorbed on the disk of OPG. Disk currents in solid lines; ring currents in dashed lines; current on OPG disk without Fe-TSP, dotted line. Electrolyte: 0.1M NaOH. Scan rate: 5m V/s. Ring potential: +0.1V vs SCE. Collection efficiency: N=0.38.

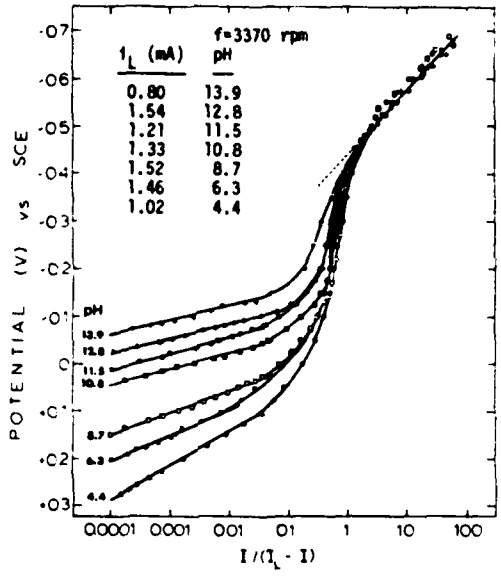

Figure 10. Tafel plots for O_2 reduction on Fe-TSP adsorbed on OPG in solution of various pH values. Rotation Rate: 3370 rpm

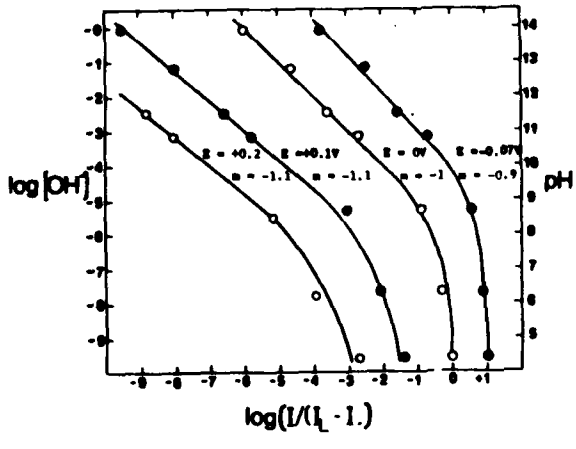

Figure 11. Plots of log $(I/(I_L-I))$ vs log (OH^-) for values of $I/(I_L-I)$ taken from the Tafel linear region of low polarization in Fig. 10 extrapolated, if necessary, at a constant potential.

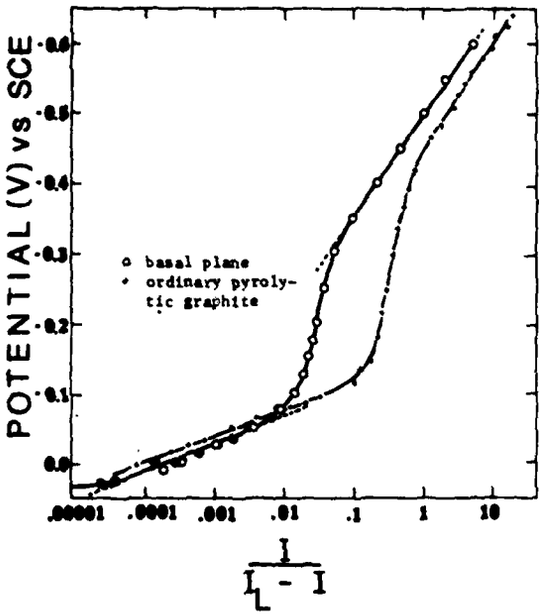

Figure 12. Tafel plot of log $(I/(I_L-I))$ vs E for O_2 reduction on Fe-TSP adsorbed on SAPG and OPG at F=3000 rpm in 0.1M NaOH.

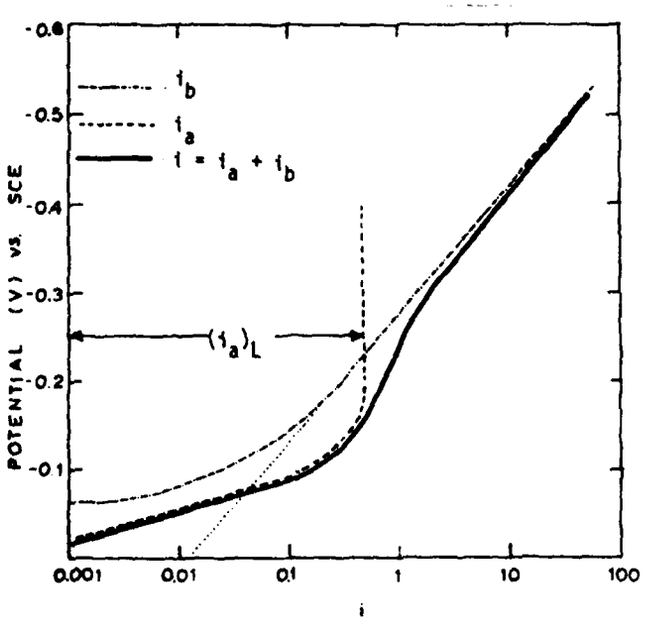

Figure 13. Graphical representation of the combination of two processes for O_2 reduction on adsorbed Fe-TSP in basic media.

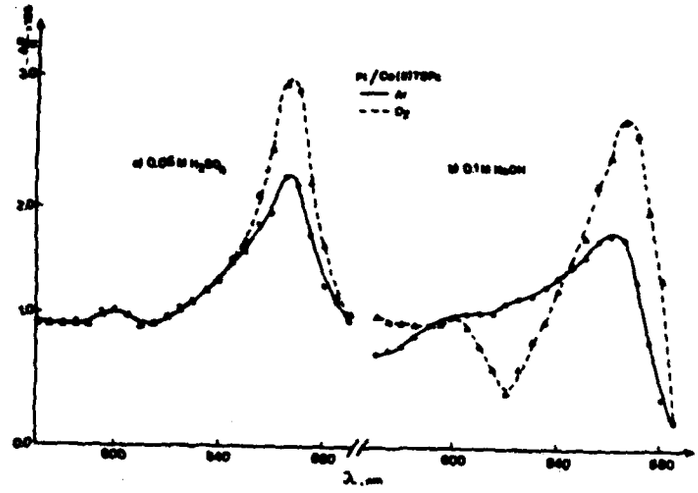

Figure 14. Reflectance spectra of Co(II)-TSP adsorbed on Pt at 0.70V vs RHE in 0.05M H_2SO_4 (a) and 0.1M NaOH (b) with argon and O_2 saturated solutions. Parallel optical polarization.

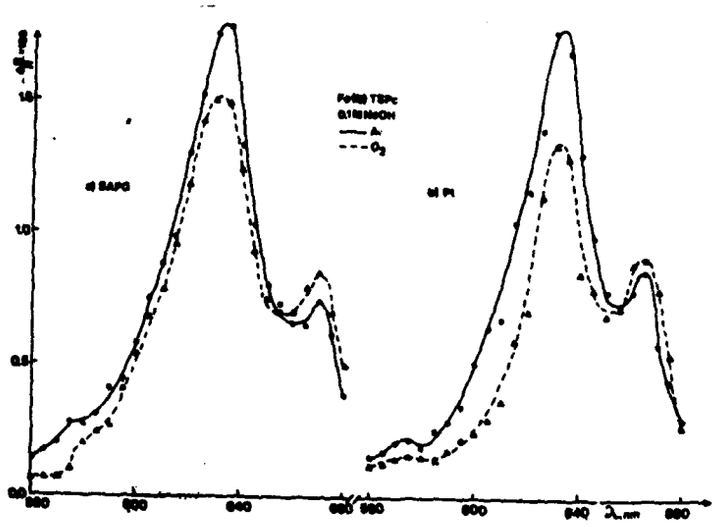

Figure 15. Reflectance spectra of Fe(III)-TSP adsorbed on basal plane of SAPG at 0.90V vs RHE (a) and on Pt at 0.70V vs RHE (b) with argon and O_2 saturated solutions. Perpendicular optical polarization.

TECHNICAL REPORT DISTRIBUTION LIST, GEN

	No. Copies
Office of Naval Research Attn: Code 472 800 North Quincy Street Arlington, Virginia 22217	2
ONR Branch Office Attn: Dr. George Sandoz 536 S. Clark Street Chicago, Illinois 60605	1
ONR Branch Office Attn: Scientific Dept. 715 Broadway New York, New York 10003	1
ONR Branch Office 1030 East Green Street Pasadena, California 91106	1
ONR Branch Office Attn: Dr. L. H. Peebles Building 114, Section D 666 Summer Street Boston, Massachusetts 02210	1
Director, Naval Research Laboratory Attn: Code 6100 Washington, D.C. 20390	1
The Assistant Secretary of the Navy (R,E&S) Department of the Navy Room 4E736, Pentagon Washington, D.C. 20350	1
Commander, Naval Air Systems Command Attn: Code 310C (H. Rosenwasser) Department of the Navy Washington, D.C. 20360	1
Defense Documentation Center Building 5, Cameron Station Alexandria, Virginia 22314	12
Dr. Fred Saalfeld Chemistry Division Naval Research Laboratory Washington, D.C. 20375	1
U.S. Army Research Office Attn: CRD-AA-IP P.O. Box 1211 Research Triangle Park, N.C. 27709	1
Naval Ocean Systems Center Attn: Mr. Joe McCartney San Diego, California 92152	1
Naval Weapons Center Attn: Dr. A. B. Amster, Chemistry Division China Lake, California 93555	1
Naval Civil Engineering Laboratory Attn: Dr. R. W. Drisko Port Hueneme, California 93401	1
Department of Physics & Chemistry Naval Postgraduate School Monterey, California 93940	1
Dr. A. L. Slafkosky Scientific Advisor Commandant of the Marine Corps (Code RD-1) Washington, D.C. 20380	1
Office of Naval Research Attn: Dr. Richard S. Miller 800 N. Quincy Street Arlington, Virginia 22217	1
Naval Ship Research and Development Center Attn: Dr. G. Bosmajian, Applied Chemistry Division Annapolis, Maryland 21401	1
Naval Ocean Systems Center Attn: Dr. S. Yamamoto, Marine Sciences Division San Diego, California 91232	1
Mr. John Boyle Materials Branch Naval Ship Engineering Center Philadelphia, Pennsylvania 19112	1

TECHNICAL REPORT DISTRIBUTION LIST, GEN

	No. Copies
Dr. Rudolph J. Marcus Office of Naval Research Scientific Liaison Group American Embassy APO San Francisco 96503	1
Mr. James Kelley DTNSRDC Code 2803 Annapolis, Maryland 21402	1

TECHNICAL REPORT DISTRIBUTION LIST, 359

	No. Copies
Dr. Paul Delahay Department of Chemistry New York University New York, New York 10003	1
Dr. E. Yeager Department of Chemistry Case Western Reserve University Cleveland, OH 44106	1
Dr. D. N. Bennion Chemical Engineering Department University of California Los Angeles, California 90024	1
Dr. R. A. Marcus Department of Chemistry California Institute of Technology Pasadena, California 91125	1
Dr. J. J. Auborn Bell Laboratories Murray Hill, New Jersey 07974	1
Dr. Adam Heller Bell Laboratories Murray Hill, New Jersey 07974	1
Dr. T. Katan Lockheed Missiles & Space Co, Inc. P.O. Box 504 Sunnyvale, California 94088	1
Dr. Joseph Singer, Code 302-1 NASA-Lewis 21000 Brookpark Road Cleveland, Ohio 44135	1
Dr. B. Brummer EIC Incorporated 55 Chapel Street Newton, Massachusetts 02158	1
Library P. R. Mallory and Company, Inc. Northwest Industrial Park Burlington, Massachusetts 01803	1
Dr. P. J. Hendra Department of Chemistry University of Southhampton Southhampton SO9 5NH United Kingdom	1
Dr. Sam Perone Department of Chemistry Purdue University West Lafayette, Indiana 47907	1
Dr. Royce W. Murray Department of Chemistry University of North Carolina Chapel Hill, North Carolina 27514	1
Naval Ocean Systems Center Attn: Technical Library San Diego, California 92152	1
Dr. C. E. Mueller The Electrochemistry Branch Materials Division, Research & Technology Department Naval Surface Weapons Center White Oak Laboratory Silver Spring, Maryland 20910	1
Dr. G. Goodman Globe-Union Incorporated 5757 North Green Bay Avenue Milwaukee, Wisconsin 53201	1
Dr. J. Boechler Electrochimica Corporation Attention: Technical Library 2485 Charleston Road Mountain View, California 94040	1
Dr. P. P. Schmidt Department of Chemistry Oakland University Rochester, Michigan 48063	1
Dr. H. Richtol Chemistry Department Rensselaer Polytechnic Institute Troy, New York 12181	1

TECHNICAL REPORT DISTRIBUTION LIST, 359

	No. Copies
Dr. A. B. Ellis Chemistry Department University of Wisconsin Madison, Wisconsin 53706	1
Dr. M. Wrighton Chemistry Department Massachusetts Institute of Technology Cambridge, Massachusetts 02139	1
Larry E. Plew Naval Weapons Support Center Code 30736, Building 2906 Crane, Indiana 47522	1
S. Ruby DOE (STOR) 600 E Street Washington, D.C. 20545	1
Dr. Aaron Wold Brown University Department of Chemistry Providence, Rhode Island 02192	1
Dr. R. C. Chudacek McGraw-Edison Company Edison Battery Division Post Office Box 28 Bloomfield, New Jersey 07003	1
Dr. A. J. Bard University of Texas Department of Chemistry Austin, Texas 78712	1
Dr. M. M. Nicholson Electronics Research Center Rockwell International 3370 Miraloma Avenue Anaheim, California	1
Dr. Donald W. Ernst Naval Surface Weapons Center Code R-33 White Oak Laboratory Silver Spring, Maryland 20910	1
Dr. R. P. Van Duyne Department of Chemistry Northwestern University Evanston, Illinois 60201	1
Dr. B. Stanley Pons Department of Chemistry Oakland University Rochester, Michigan 48063	1
Dr. Michael J. Weaver Department of Chemistry Michigan State University East Lansing, Michigan 48824	1
Dr. R. David Rauh EIC Corporation 55 Chapel Street Newton, Massachusetts 02158	1
Dr. J. David Margerum Research Laboratories Division Hughes Aircraft Company 3011 Malibu Canyon Road Malibu, California 90265	1
Dr. Martin Fleischmann Department of Chemistry University of Southampton Southampton 509 5NH England	1
Dr. Janet Osteryoung Department of Chemistry State University of New York at Buffalo Buffalo, New York 14214	1
Dr. R. A. Osteryoung Department of Chemistry State University of New York at Buffalo Buffalo, New York 14214	1
Mr. James R. Moden Naval Underwater Systems Center Code 3632 Newport, Rhode Island 02840	1

TECHNICAL REPORT DISTRIBUTION LIST, 359

	No. Copies
Dr. R. Nowak Naval Research Laboratory Code 6130 Washington, D.C. 20375	1
Dr. John F. Houlihan Shenango Valley Campus Penn. State University Sharon, PA 16146	1